Oil & Gas Science and Technology – Rev. IFP, Vol. 62 (2007), No. 1, pp. 79-89

DOI: 10.2516/ogst:2007007

Dossier

Recent Advances in the Analysis of Catalysts and Petroleum Products
Avancées récentes en analyse des catalyseurs et des produits pétroliers

X-ray Photoelectron Spectroscopy Surface Quantification of Sulfided CoMoP Catalysts

Relation Between Activity and Promoted Sites

Part I: Influence of the Co/Mo Ratio

A.D. Gandubert[1], C. Legens[1], D. Guillaume[1], S. Rebours[1] and E. Payen[2]

1 Institut français du pétrole, IFP-Lyon, BP3, 69390 Vernaison - France
2 Unité de Catalyse et Chimie des Solides, Université des Sciences et Technologies de Lille, Bat C3, 59650 Villeneuve d'Ascq - France
e-mail: annegan78@yahoo.fr - christelle.legens@ifp.fr - denisjm.gillaume@ifp.fr - edmond.payen@univ-lille1.fr - Stephane.rebours@ifp.fr

Résumé — Quantification de surface de catalyseurs sulfures de type CoMoP par spectroscopie de photoélectrons X – Relation entre activité et sites promus – Partie I : Influence du rapport Co/Mo — Ce travail est dédié à la caractérisation de catalyseurs d'hydrotraitement CoMoP/Al_2O_3. Afin d'identifier l'environnement du cobalt et du molybdène, la spectroscopie de photoélectrons X (XPS), la microscopie électronique à transmission (MET) et les mesures d'activité ont été utilisées. En effet une approche quantitative de la caractérisation par XPS a été développée dans le cas de catalyseurs d'hydrotraitement de type CoMoP afin d'étudier l'effet du rapport atomique Co/Mo. Nous avons quantifié les différentes espèces présentes à la surface des catalyseurs et montré que le catalyseur présentant à la fois une activité maximale en hydrogénation du toluène et une concentration maximale de phase active mixte de type CoMoS, correspond au catalyseur de rapport atomique Co/Mo nominal de 0.5. Cependant la totalité des ions cobalt n'est pas engagée dans la phase mixte CoMoS.

Abstract — X-ray Photoelectron Spectroscopy Surface Quantification of Sulfided CoMoP Catalysts – Relation Between Activity and Promoted Sites – Part I: Influence of the Co/Mo Ratio — *This work is dedicated to the characterization of CoMoP/Al_2O_3 hydrotreatment catalysts. In order to identify the neighboring of cobalt and molybdenum, X-ray photoelectron spectroscopy (XPS), transmission electron spectroscopy (TEM) and activity measurements were used. Indeed, a quantitative XPS characterization was developed to study the effect of the Co/Mo atomic ratio on CoMoP-type hydrodesulfurization catalysts. Identification and quantification of the various species present on the surface of the catalysts were performed. We showed that the catalyst exhibiting both the maximum activity in hydrogenation of toluene and the maximum amount of CoMoS active, determined through the XPS quantitative analysis, is the catalyst with a Co/Mo atomic ratio equal to 0.5. However, all the cobalt atoms are not completely engaged in the CoMoS mixed phase.*

INTRODUCTION

Hydrotreatment, a process that is required to eliminate sulfur impurities from petroleum fractions, is a catalytic process that uses CoMoP- or NiMoP-type catalysts. On an atomic scale their active phases consist of molybdenum disulfide slabs promoted by cobalt or nickel atoms that are well dispersed on a high specific area alumina. These CoMoS (NiMoS) active phases are obtained by sulfidation of an oxidic precursor that is prepared by impregnation of the alumina support with impregnation solution containing the elements to be deposited. According to Topsøe's model, cobalt atoms are located in substitution of molybdenum inside or at the edges of the MoS_2 nanoparticles [1]. In the same way, theoretical DFT calculation showed that the most favorable localization of the promoter (cobalt or nickel) was found for the substitution of the molybdenum atoms by cobalt (or nickel) atoms located at the edges of the MoS_2 slabs [2].

As the highest sulfur content allowed in gasoline and diesel is continually decreasing, more and more efficient hydrotreatment catalysts are required. Improvement of these catalysts requires a better understanding of the structure and genesis of these CoMoS phases. Thus, a procedure to characterize these active phases has been established. In this context, a multi-techniques approach correlating X-ray photoelectron spectroscopy (XPS) and transmission electron microscopy (TEM) with activity measurements was conducted. In particular, we elaborated a process to determine and quantify each chemical cobalt and molybdenum species present on the surface of the sample with the XPS technique. This was obtained thanks to the study of the binding energies (BE) of reference catalysts and the measurement of XPS peak intensities relative to each species defined previously. By using the techniques of characterization mentioned above, the objective of this work was to study the effect of the Co/Mo atomic ratio of CoMoP-type catalysts on the formation of the CoMoS active phase. Indeed, the catalysts used in this work have rarely been studied as they are synthesized by a new way of preparation. Addition of phosphorus to the catalytic formulations of hydrodesulfurization catalysts has been recognized as a way to improve their catalytic performances, and different methods of introduction have been proposed [3-5]. One of the most efficient starting impregnation solutions is based on the synthesis of $P_2Mo_5O_{23}(Co_x)$ heteropolycompounds, which permits the preparation of high Mo loading catalysts. However, optimization of its formulation has rarely been performed.

1 EXPERIMENTAL SECTION

1.1 Catalyst Preparation

The oxidic precursors were prepared by incipient wetness impregnation of γ-alumina extrudates (from *Axens*) with impregnation solutions containing the appropriate amount of metal to be deposited. The impregnated extrudates were then placed in a water-saturated atmosphere for at least three hours and then dried at 120°C overnight. Finally, the solids were calcined under air at 500°C for two hours. The bimetallic CoMoP-type catalysts with various Co/Mo ratios were prepared with impregnation solutions obtained by dissolving molybdenum oxide -MoO_3- and cobalt hydroxide -$Co(OH)_2$- in a phosphoric acid aqueous solution [3]. A large excess of phosphoric acid, corresponding to 6 wt% P_2O_5 loading, was necessary to dissolve the molybdenum and cobalt precursors well. The Mo loading was 20 wt% as MoO_3, and the concentration of Co was adjusted to obtain various Co/Mo atomic ratios. These oxidic catalysts will be referred to as *CoMoP(X)-ox*, where *X* represents the Co/Mo atomic ratio. The Co loadings correspond to 1.1, 2.2, 3.3, 4.6, 5.6, 6.7 and 7.8 wt% CoO for, respectively, 0.1, 0.2, 0.3, 0.4, 0.5, 0.6 and 0.7 ratios.

Three monometallic samples, prepared according to the same method, were used as references for XPS spectra interpretations: one containing only cobalt, one containing only molybdenum and one composed of molybdenum doped by phosphorus. The impregnation solutions were prepared by dissolving cobalt hydroxide $Co(OH)_2$ in a sulfuric acid aqueous solution, ammonium heptamolybdate $(NH_4)_6Mo_7O_{24}$ in water, and molybdenum oxide MoO_3 in a phosphoric acid aqueous solution [3], for, respectively, the Co-, the Mo- and MoP-type catalysts that will be hereafter referred to as *Co*, *Mo* and *MoP*, respectively. The metal loadings were 5.6 wt% as CoO for the *Co* sample and 20 wt% as MoO_3 for the *Mo* and *MoP* solids. For each sample, the nomenclature, the theoretical composition and the experimental concentrations determined by the X-ray fluorescence technique are listed in Table 1.

1.2 Sulfidation Conditions

The oxide precursors were sulfided under a H_2S/H_2 (15-85%) mixture with a gas flow at atmospheric pressure of 2 L/h/g of catalyst. The samples were heated under the sulfiding mixture at a rate of 5°C/min up to 400°C and maintained at this temperature for two hours. They were then cooled down to room temperature at a rate of 20°C/min, also under the reactive mixture. The sulfided catalysts were transferred into glass vials under vacuum in order to avoid any contact with air. The nomenclature of the sulfided samples will be the same as the oxidic ones, with *-S* instead of *-ox*. The oxide references were sulfided as well.

1.3 XPS Analysis

The XPS sampling of the sulfided catalysts was performed in a glove box under argon atmosphere, with controlled oxygen and water levels (less than 20 ppm) in order to avoid their

TABLE 1

Composition of the oxide catalysts (**theo.** represents the theoritical loadings, **exp.** corresponds to the loading determined by X-ray fluorescence)

Catalyst code	**MoO_3 loading**		**CoO loading**		**P_2O_5 loading**		**Co/Mo atomic ratio**	
	theo. (wt %)	**exp. (wt % ± 0.27)**	**theo.**	**exp. (wt % ± 0.07)**	**theo.**	**exp. (wt % ± 0.04)**	**theo.**	**exp.**
Co-ox	/	/	5.6	5.20	/	/	/	**/**
Mo-ox	20.0	20.74	/	/	/	/	/	**/**
MoP-ox	20.0	20.76	/	/	6.0	5.18	/	**/**
CoMoP(0.1)-ox	20.0	20.17	1.1	0.97	6.0	5.26	0.10	**0.09**
CoMoP(0.2)-ox	20.0	20.24	2.2	2.04	6.0	5.21	0.20	**0.19**
CoMoP(0.3)-ox	20.0	19.44	3.3	2.95	6.0	5.05	0.30	**0.30**
CoMoP(0.4)-ox	20.0	20.48	4.6	4.34	6.0	5.13	0.40	**0.41**
CoMoP(0.5)-ox	20.0	20.20	5.6	4.89	6.0	5.98	0.50	**0.47**
CoMoP(0.6)-ox	20.0	19.09	6.7	5.91	6.0	5.42	0.60	**0.60**
CoMoP(0.7)-ox	20.0	18.17	7.8	6.39	6.0	5.10	0.70	**0.68**

partial reoxidation. The samples were crushed and pressed onto an indium foil that was attached to the sample holder via a double-sided carbon tape. The sample holder was then moved directly to the introduction chamber of the XPS spectrometer, thanks to the special connection of the glove box to the XPS spectrometer. The XPS spectra were recorded on a KRATOS AXIS ULTRA instrument with Al monochromator source (1486.6 eV) and a hemi-spherical analyzer operating at fixed pass energy of 40 eV. The measurements were made at 293 K in steps of 0.05 eV for cobalt and 0.1 eV for molybdenum, and at a pressure lower than $1{\cdot}10^{-9}$ Pa in the sample analysis chamber. Binding energies (BE) of the various elements were referenced to the C1s level of the contamination carbon at 284.6 eV. The curves were integrated by applying a Shirley-type baseline. The collected spectra were analyzed by using CasaXPS software, Version 2.0.71 [6]. The decomposition of the Mo3d and Co2p XPS spectra were performed using the appropriate oxide and sulfided references as supported monometallic catalysts defined before and with an unsupported MoS_2 compound. Analysis of the Mo3d spectrum gives the sulfidation rate into MoS_2, whereas the Co2p spectrum allows us to quantify the amount of the CoMoS phase. The methodology developed to decompose the spectra will be detailed hereafter.

The quantification of metallic atoms was obtained from the measurement of the corresponding peak area and the use of relative sensitivity factors (RSF), particular to the spectrometer and furnished by the manufacturer. To approach the effective atomic surface concentrations, all the atoms (except the contamination carbon) detected on the surface were taken into account.

For one atom, the signal obtained can be decomposed into different contributions relative to various chemical species. The calculation of the respective contribution of each peak area will lead to the knowledge of the relative proportion of each chemical form for a given atom. Two samples were analyzed for each catalyst and the data presented correspond to the average values of the two analyses. The relative error is estimated to be ±10%.

1.4 TEM Analysis

The sulfided samples were analyzed by TEM to determine the average length and stacking of the MoS_2 slabs by counting at least 350 particles. The extrudates were crushed into a fine powder, a small amount of which was ultra-sonically diluted in ethanol. Two drops of this solution were deposited on a carbon-coated Cu grid and the solvent was evaporated under infrared light. TEM images were taken using a 200 kV JEOL-2010 transmission electron microscope equipped with a digital camera.

1.5 Activity Measurements

The sulfided samples were tested in toluene hydrogenation in hydrotreatment conditions. The catalytic tests were carried out in a fixed bed high-pressure flow microreactor under the following conditions: 2 cm^3 of crushed extrudates (300-1000 μm) diluted in SiC, total pressure of 60 MPa, reaction temperature of 350°C, liquid hourly space velocity (LHSV) of 2 h^{-1}, hydrogen-to-feed ratio of 450 L/L. The feed consists of dimethyldisulfide (5.9 wt%) and toluene (20 wt%) mixture in cyclohexane. After the unit was pressure-tested at room temperature, the temperature was increased at 3°C/min to 350°C. Steady-state conversion was measured after 2 hours onstream. Reaction products were analyzed by online gas chromatography. The activity in toluene hydrogenation was expressed considering a first-order reaction.

2 RESULTS AND DISCUSSION

2.1 XPS Characterization

Quantitative analysis of the various species present on the surface of sulfided catalysts requires first an identification of these species, which then permits a decomposition of the spectra in order to access the relative amount of each one. The spectra were therefore all recorded with the same analytical parameters for the catalysts and the reference solids. For each chemical species, the XPS spectral envelope was decomposed into a main peak and associated ones, these latter being fully linked to the main peak via their binding energy, full width at half maximum (FWHM) and relative area. Moreover, corrections were applied to the binding energy and to the FWHM of the main peak (and as a consequence of the associated ones) in order to take into account the charge effect, which was performed by reference, respectively, to the C1s and Al2p peaks.

2.1.1 Cobalt Species

Previous studies on pure chromium [7] or iron [8] compounds have shown the necessity to combine theoretical modeling calculations with experimental XPS results to describe as well as possible the main core level. The aim of this study is not to describe in detail the Co2p core line spectrum by assigning multiplet splitting and shake up appropriate binding energies with respect to the chemical environment of the cobalt atom, but to define the relative amount of each species supposed to be on the alumina support, assuming that they do not alter from one sample to another. We will therefore assume that the parts of the spectrum defined as $Co2p_{3/2}$ and $Co2p_{1/2}$ main peaks include some of the multiplet splitting contributions.

The fitting of the Co2p XPS peaks was realized in three steps that are, for a better understanding of the method, detailed below in the case of the *CoMoP(0.3)-S* catalyst. The first step consists of determining the oxide signature of the cobalt species. Figure 1 shows the spectrum of the *CoMoP(0.3)-ox* solid. We determined the spectral envelope of the cobalt spectrum as composed of two main peaks corresponding to $Co2p_{3/2}$ and $Co2p_{1/2}$ contributions with their corresponding satellites (blue peaks). The $Co2p_{3/2}$ and $Co2p_{1/2}$ main binding energies are observed at 781.5 ± 0.1 eV and 797.3 ± 0.1 eV, respectively, and the FWHM ratio between $Co2p_{3/2}$ and Al2p peaks is 1.3. Similar values were observed for the monometallic *Co-ox* sample. This ratio, as well as the binding energy of the main peaks and the constraints applied to the satellites, will be maintained for all the cobalt spectra decompositions including a cobalt oxide contribution. These constraints in position, the area and FWHM relative to the main peak are gathered in Table 2.

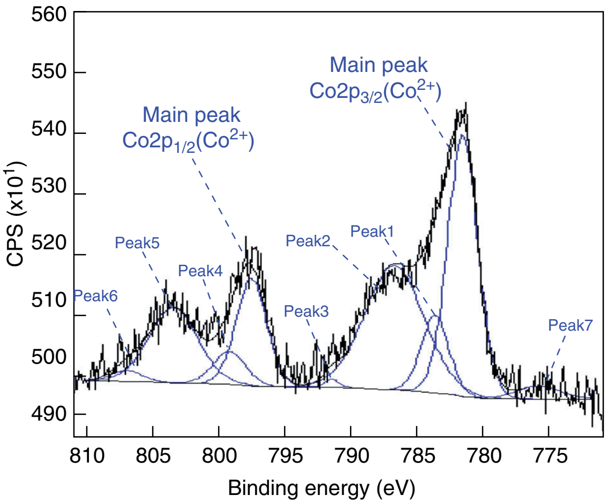

Figure 1

XPS Co2p spectrum of the bimetallic *CoMoP(0.3)-ox* (in blue: Co^{2+} oxide contributions).

TABLE 2

XPS processing parameters used to describe the cobalt oxide Co^{2+} contributions

($^{\#}$ FWHM referenced to the FWHM of the Al2p peak, with a Co/Al ratio of 1.3)

	Co^{2+} PHASE		
Contribution	**Binding energy (± 0.10 eV)**	**Peak area**	**FWHM (± 0.10 eV)**
Main peak $Co2p_{3/2}$	781.51 (A)	B	C $^{\#}$
Main peak $Co2p_{1/2}$	797.36 (A + 15.85)	B * 0.42	C * 1.02
Peak1	A + 2.07	B * 0.27	C * 0.92
Peak2	A + 5.12	B * 0.94	C * 1.97
Peak3	A + 9.92	B * 0.01	C * 0.49
Peak4	A + 17.50	B * 0.14	C * 1.08
Peak5	A + 21.72	B * 0.47	C * 1.62
Peak6	A + 25.20	B * 0.04	C * 0.99
Peak7	A - 4.27	B * 0.12	C * 1.46

The binding energy of the main peak ($Co2p_{3/2}$) does not permit differentiation of cobalt^{2+} from cobalt^{3+} in an oxide environment. On the contrary, the presence of an intense peak at 786.8 eV (peak 2 in *Fig. 1*) and the lack of a peak at about 791 eV (weak peak 3 in *Fig. 1*) characteristic of cobalt^{3+} points out that the oxide cobalt species corresponds only to cobalt^{2+}, as was already observed by Martin *et al.* [9].

In a second step we determined the binding energy of the surface cobalt sulfide. Figure 2 shows the XPS spectrum of

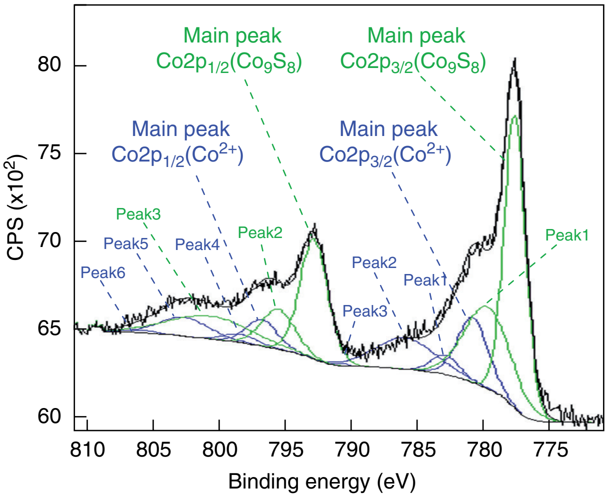

Figure 2

XPS Co2p spectrum of the monometallic *Co-S* (in blue: Co^{2+} oxide contributions; in green: Co9S8 contributions).

the *Co-S* sample in which we can also identify the aforementioned oxide Co2p features, in agreement with the literature data. Indeed, it is well recognized that it is difficult to obtain a complete sulfidation. Decomposition into sulfide and oxide components was therefore performed by introducing the oxide Co^{2+} contributions with the constraints defined above. This allows us to deduce the spectrum characteristic of the sulfide species present on the alumina surface after sulfidation, the main binding energies of which being at 778 ± 0.1 eV and 793.2 ± 0.1 eV for the $Co2p_{3/2}$ and $Co2p_{1/2}$ levels, respectively. These values correspond to those observed for Co_9S_8 by reference to the literature data [9-11]. As for the determination of the oxide contribution decomposition, constraints were determined to the binding energies, the areas and the FWHM for the Co_9S_8 peaks, relatively to the main $Co2p_{3/2}$ (Co_9S_8) peak. Moreover, the FWHM of $Co2p_{3/2}$ was referred to the FWHM of the Al2p peak, their ratio being close to 1. These parameters, used for the $Co2p_{1/2}$ peak and the satellite decomposition, are gathered in Table 3 and will be used to decompose all the spectra, including Co_9S_8 contributions.

These data now allow us to perform the decomposition of the spectrum of the bimetallic catalyst *CoMoP(0.3)-S*. Figure 3 shows the three different contributions that were extracted. Taking into account the two aforementioned Co oxide (blue peaks) and sulfide (green peaks) species, we thus deduce the contribution of the CoMoS phase (red peaks) with the two main peaks at 778.7 ± 0.1 eV and 793.6 ± 0.1 eV. Similarly, the decompositions of the $Co2p_{1/2}$ peak and satellites were performed using the constraints reported in Table 4. These constraints will be used for the processing of all the spectra containing a CoMoS phase contribution. We observed on all the samples that the FWHM ratio to Al2p is stable at 0.9.

TABLE 3

XPS processing parameters used to describe the cobalt sulfide Co_9S_8 phase contributions
($^\#$ FWHM referenced to the FWHM of Al2p peak, with a Co/Al ratio of 1.0)

Co_9S_8 PHASE			
Contribution	**Binding energy (± 0.10 eV)**	**Peak area**	**FWHM (± 0.10 eV)**
Main peak $Co2p_{3/2}$	778.09 (G)	H	I $^\#$
Main peak $Co2p_{1/2}$	793.00 (G + 14.91)	H * 0.53	I * 1.30
Peak1	G + 2.04	H * 0.60	I * 2.16
Peak2	G + 17.78	H * 0.21	I * 1.56
Peak3	G + 22.99	H * 0.30	I * 3.80

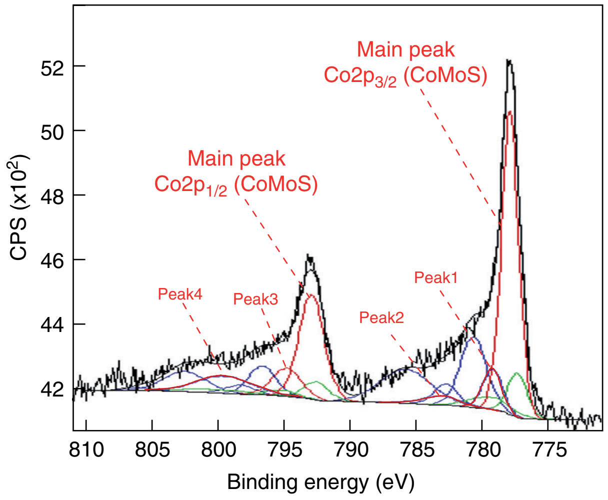

Figure 3

XPS Co2p spectrum of the bimetallic *CoMoP(0.3)-S* (in blue: Co^{2+} oxide contributions; in green: Co_9S_8 contributions; in red: CoMoS mixed phase contributions).

The difference between the binding energies of the $Co2p_{3/2}$ peak and the $Mo3d_{5/2}$ peak of the CoMoS phase (the decomposition of molybdenum spectra is presented in the next paragraph), ΔBE[Co2p-Mo3d], is equal to 549.6 eV and the difference between the binding energies of the $Co2p_{3/2}$ peak of the CoMoS phase and the $S2p_{3/2}$ peak of the sulfide phase (BE measured at 161.6 ± 0.1 eV), ΔBE[Co2p-S2p], is equal to 617.1 eV. Both of these values are in good agreement with the literature data and confirm the CoMoS nature of this phase [9-12].

All the Co2p spectra of the CoMoP catalysts were processed by using this method and by applying the processing constraints presented in Table 2 for the oxide phase,

TABLE 4

XPS processing parameters used to describe the CoMoS mixed phase contributions (# FWHM referenced to the FWHM of Al2p peak, with a Mo/Al ratio of 0.9)

CoMoS PHASE			
Contribution	**Binding energy (± 0.10 eV)**	**Peak area**	**FWHM (± 0.10 e**
Main peak $Co2p_{3/2}$	778.64 (D)	E	F #
Main peak $Co2p_{1/2}$	793.55 (D + 14.91)	E * 0.50	F * 1.45
Peak1	D + 1.31	E * 0.15	F * 1.13
Peak1	D + 5.15	E * 0.06	F * 2.26
Peak2	D + 16.77	E * 0.15	F * 1.66
Peak3	D + 21.53	H * 0.18	F * 3.17

Table 3 for the sulfide phase and 4 for the CoMoS mixed phase. These decompositions of cobalt spectra will allow us to follow the quantitative evolution of cobalt species for the CoMoP catalysts with various Co/Mo atomic ratios.

2.1.2 Molybdenum Species

Similar decomposition of the Mo3d XPS peaks was performed using reference XPS spectra, as shown below for the *CoMoP(0.3)-S* catalysts. The methodology developed to decompose the molybdenum spectra was the same as for cobalt and the constraints applied for the processing of each spectrum are presented in Tables 5, 6 and 7. Figure 4 shows the spectrum of the oxide *CoMoP(0.3)-ox* catalyst that is characteristic of Mo^{6+} in an oxygen environment [10, 13]. The $Mo3d_{5/2}$ and Mo $3d_{3/2}$ binding energies are observed at 233 ± 0.1 eV and 236.1 ± 0.1 eV, respectively (blue peaks). This spectrum was used as reference for the decomposition of the *CoMoP(0.3)-S*. However, we observed that for the decomposition of the sulfided sample, a shift from 233 eV to 232 eV for the Mo^{6+} contribution was necessary to fit the spectrum well. This has already been reported in the literature and was explained as a less oxidizing environment next to the molybdenum consecutively to the transformation of most oxidic Mo into MoS_2 [16].

The contribution of molybdenum sulfide is determined by analyzing an unsupported reference MoS_2. The binding energies of $Mo3d_{5/2}$ and $Mo3d_{3/2}$ peaks are, respectively, 229.1 ± 0.1 eV and 232.2 ± 0.1 eV, as shown in Figure 5 (red peaks).

These data now allow us to perform the decomposition of the spectrum of the bimetallic catalyst *CoMoP(0.3)-S*. Figure 6 shows the three different contributions that were extracted, taking into account the two aforementioned Mo^{6+} oxide (blue peaks) and MoS_2 (red peaks) species. However, the fitting requires another contribution that may correspond to molybdenum oxysulfide MoS_yO_x species (green peaks) as often suggested in the literature [11, 14, 15], the characteristic binding energies being 229.8 eV and 232.9 eV for $Mo3d_{5/2}$ and $Mo3d_{3/2}$, respectively.

All the Mo3d spectra were processed by using this method and by applying the processing constraints reported in Table 5 for the oxide phase, Table 6 for the sulfide phase and Table 7 for the oxysulfide phase.

TABLE 5

XPS processing parameters used to describe the molybdenum oxide Mo^{6+} contributions (# FWHM referenced to the FWHM of Al2p peak, with a Mo/Al ratio of 1.1)

Mo^{6+} PHASE			
Contribution	**Binding energy (± 0.10 eV)**	**Peak area**	**FWHM (± 0.10 eV)**
$Mo3d_{5/2}$	233.00 (A)	B	C #
$Mo3d_{3/2}$	A + 3.15	B * 0.62	C * 0.94

TABLE 6

XPS processing parameters used to describe the molybdenum sulfide phase contributions (# FWHM referenced to the FWHM of Al2p peak, with a Mo/Al ratio of 0.6)

MoS_2 PHASE			
Contribution	**Binding energy (± 0.10 eV)**	**Peak area**	**FWHM (± 0.10 eV)**
MoS_2 $3d_{5/2}$	229.10 (D)	E	F #
MoS_2 $3d_{3/2}$	D + 3.15	E * 0.68	F * 1.21

TABLE 7

XPS processing parameters used to describe the molybdenum oxysulfide phase contributions (# FWHM referenced to the FWHM of Al2p peak, with a Mo/Al ratio of 0.9)

MoS_xO_y PHASE			
Contribution	**Binding energy (± 0.10 eV)**	**Peak area**	**FWHM (± 0.10 eV)**
MoS_xO_y $3d_{5/2}$	229.84 (G)	H	I #
MoS_xO_y $3d_{3/2}$	G + 3.15	H * 0.62	I * 0.94

2.1.3 Quantification of the Cobalt and Molybdenum Species

Based on the above described decomposition of the XPS spectra, we determined the relative concentrations of each species, Co^{2+}, Co_9S_8, CoMoS, Mo^{6+}, MoS_xO_y and MoS_2, for all the sulfided CoMoP catalysts. For instance, the relative

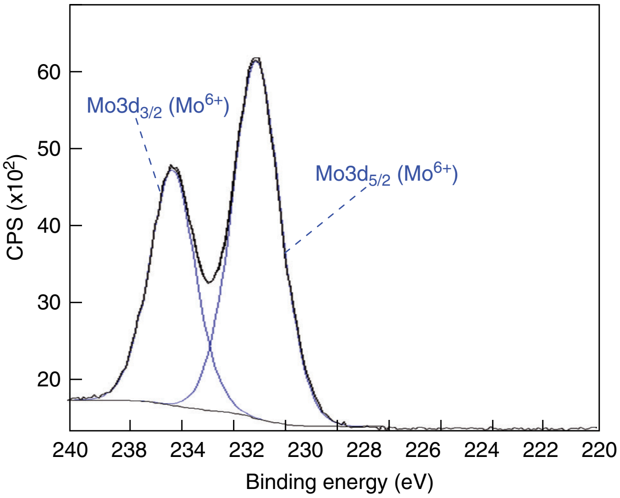

Figure 4

XPS Mo3d spectrum of the bimetallic *CoMoP(0.3)-ox* (in blue: Mo^{6+} oxide contributions).

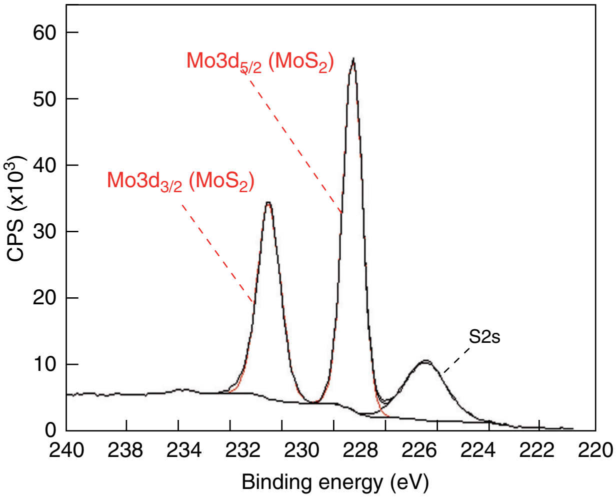

Figure 5

XPS Mo3d spectrum of unsupported MoS_2 compound (in red: MoS_2 contributions).

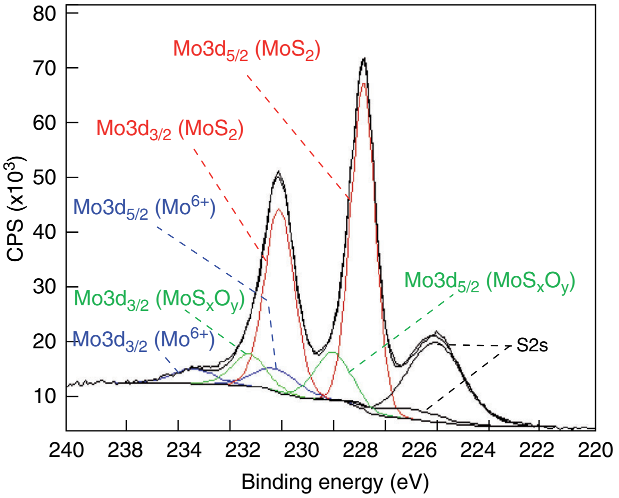

Figure 6

XPS Mo3d spectrum of the bimetallic *CoMoP(0.3)-S* (in blue: Mo^{6+} oxide contributions; in green: MoS_xO_y oxysulfide contributions; in red: MoS_2 contributions).

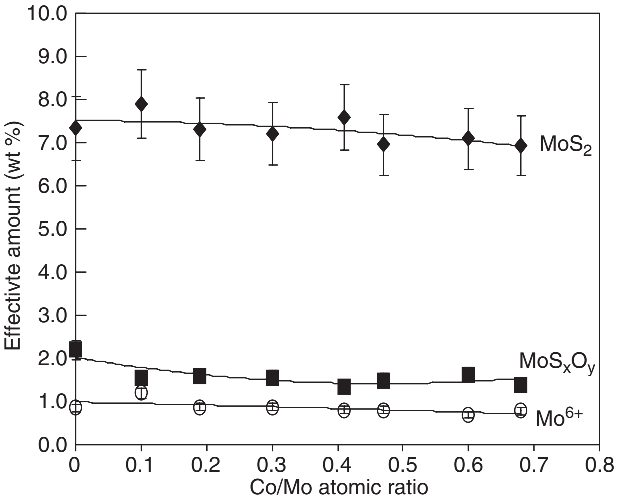

Figure 7

Effective amount of molybdenum species in relation to the Co/Mo ratio, expressed in weight percent, determined by XPS, for the CoMoP catalysts (open circle: Mo^{6+}; closed square: MoS_xO_y oxysulfide; closed diamond shape: MoS_2).

amount of the CoMoS phase, [CoMoS], was determined by using the following equation:

$$[\mathrm{CoMoS}] = \frac{I(\mathrm{CoMoS}) \times 100}{I(\mathrm{Co}^{2+}) + I(\mathrm{Co}_9S_8) + I(\mathrm{CoMoS})}$$

where I(x) represents the peak area of the species (x).

We can also approach the effective concentration of Co and Mo elements by a complete quantification of all the atoms detected, using appropriate sensitivity factors. Then we can access the effective concentrations of the species. For instance, the effective concentration of the CoMoS phase, C(CoMoS), was calculated by using the following equation:

$$C(\mathrm{CoMoS}) = [\mathrm{CoMoS}] \times C(\mathrm{Co_{tot}})$$

where $C(\mathrm{Co_{tot}})$ represents the effective concentration of cobalt determined by XPS.

2.2 XPS Results for the CoMoP-Type Catalysts with Various Co/Mo Atomic Ratios

Similar decompositions were performed for the solids with various Co/Mo ratios, and the amount of each species present in these solids after sulfidation was determined.

2.2.1 Molybdenum Species

Figure 7 shows the evolution of the effective amount of each molybdenum species, namely Mo^{6+} oxide type, MoS_xO_y oxysulfide and MoS_2 sulfide, versus the Co/Mo atomic ratio for the sulfided CoMoP catalysts. It shows that the Co/Mo ratio has no influence on the evolution of the molybdenum species. Indeed, whatever the Co/Mo ratio, between 0.0 and 0.7, the amount of residual oxide Mo^{6+}, oxysulfide MoS_xO_y and sulfide MoS_2 does not change, about 75% of the molybdenum oxide being transformed into MoS_2 upon sulfidation.

2.2.2 Cobalt Species

Figure 8 presents the evolution of the effective amount of cobalt species of the sulfided CoMoP catalysts. It shows that the amount of each cobalt species varies with the Co/Mo ratio, the amount of the CoMoS mixed phase reaching a maximum for Co/Mo ratios between 0.4 and 0.6. For these three catalysts about 50% to 60% of the Co, which corresponds to about 2.2 wt%, is engaged in the CoMoS phase, the amount of residual oxide increasing weakly with the Co/Mo ratio. It also shows that the Co_9S_8 amount increases greatly at high cobalt loading (*CoMoP(0.6)-S* and *CoMoP(0.7)-S*), which means that the additional cobalt is not in a decoration position.

2.2.3 Co/Mo Atomic Ratio of the MoS_2 Slabs

The XPS spectra processing also allowed us to determine the XPS Co/Mo atomic ratio of the promoted slabs of the CoMoS phase. This Co/Mo ratio was calculated as the ratio between the amount of cobalt engaged in the CoMoS phase and the amount of molybdenum in MoS_2 slabs. Figure 9 presents a comparison between the formal Co/Mo atomic ratio, which is defined by the Co/Mo ratio corresponding to the stoechiometry of the impregnation solution used to prepare the oxide catalysts, and the XPS Co/Mo atomic ratio of the promoted MoS_2 slabs calculated from the XPS data.

For the catalysts with a Co/Mo ratio lower than 0.5, the XPS Co/Mo ratio of the promoted slabs (CoMoS phase) is the same as the global theoretical one. It increases with the Co loading, reaching a plateau for Co/Mo = 0.5, which suggests that Co/Mo of 0.5 corresponds to the maximum amount of cobalt able to decorate the MoS_2 slabs in the sulfidation conditions used for this study.

2.3 TEM Results

All the sulfided catalysts were analyzed by TEM in order to control the dispersion of the MoS_2 platelets, and also to determine their morphology. A typical micrograph is shown in Figure 10. For all the samples the MoS_2 phase consists of more or less stacked slabs with various lengths. The histogram obtained for the *CoMoP(0.5)-S* is given in Figure 11. Figure 12 presents the average length of MoS_2 slabs of the sulfided CoMoP catalysts versus the Co/Mo ratio. Whatever the Co/Mo ratio, the MoS_2 slabs have approximately the same length, around 34 Å, and the stacking is around 1.9 slabs, as shown in Figure 13.

2.4 Comparison Between XPS and TEM Results

XPS analysis showed that the *CoMoP(0.5)-S* and *CoMoP(0.6)-S* have the maximum amount of the mixed CoMoS active phase. Moreover, the Co/Mo ratio of the slabs

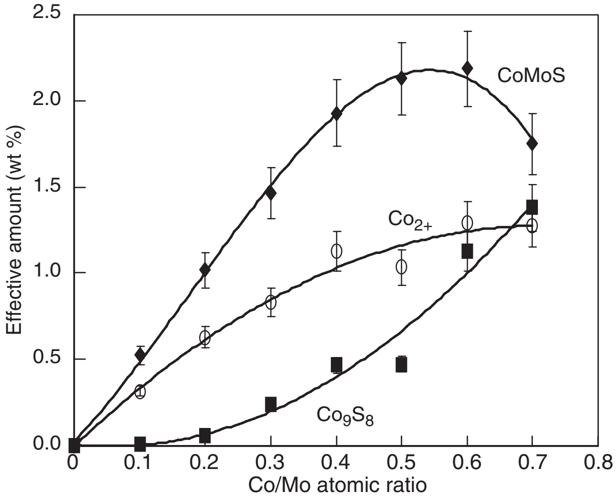

Figure 8

Effective amount of cobalt species in relation to the Co/Mo ratio, expressed in weight percent, determined by XPS, for the CoMoP catalysts (open circle: Co^{2+} oxide; closed square: Co_9S_8; closed diamond shape: CoMoS mixed phase).

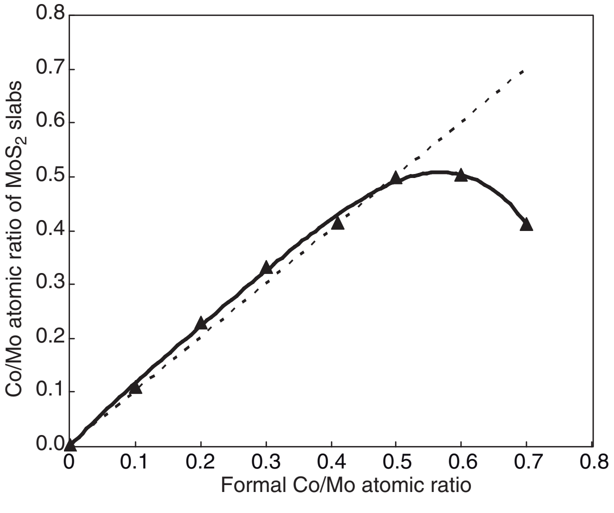

Figure 9

Comparison between theoretical Co/Mo ratio and Co/Mo ratio of the promoted MoS_2 slabs determined by XPS, for the CoMoP catalysts.

Figure 10

Transmission electron microscopy micrograph of the *CoMoP(0.5)-S* catalyst.

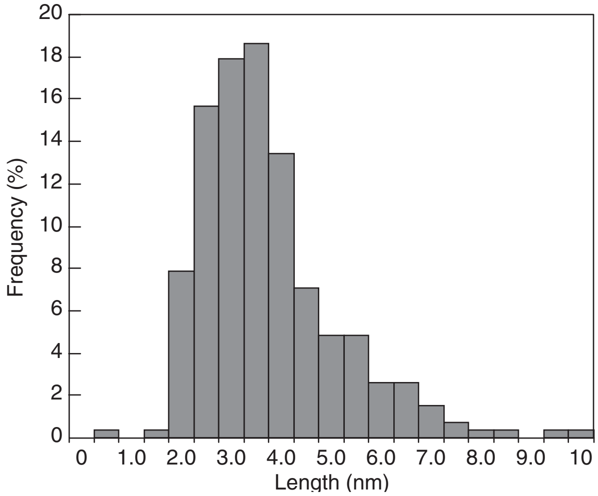

Figure 11

Histogram of the length of MoS_2 slabs realized from the analysis of the *CoMoP(0.5)-S* by TEM.

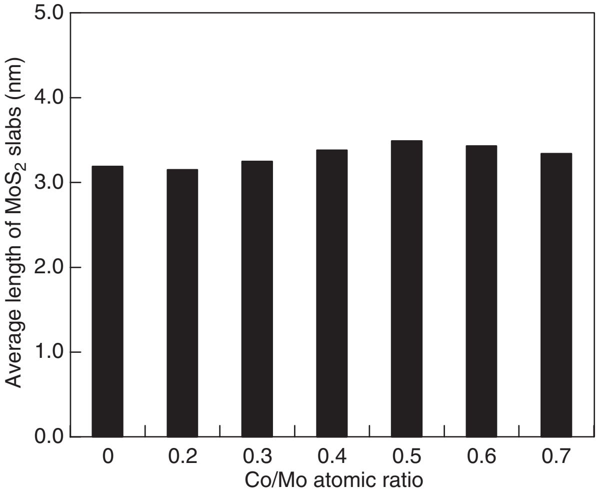

Figure 12

Average length of MoS_2 slabs determined by TEM, for the sulfided CoMoP catalysts at various Co/Mo ratios.

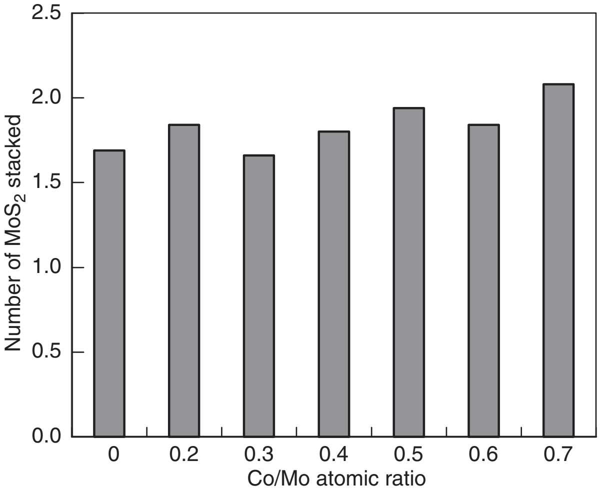

Figure 13

Average number of stacked MoS_2 slabs determined by TEM, for the sulfided CoMoP catalysts at various Co/Mo ratios.

is the same as the global Co/Mo ratio of the catalyst, equal to 0.5. Taking into account the geometrical model proposed by Kasztelan based on a total substitution of Mo located at the edges and corners of the slabs by Co atoms [17], this ratio should correspond to MoS_2 slabs of 32 Å long, a value in good agreement with the TEM measurements. On the contrary, for the *CoMoP(0.7)-S* the XPS analysis showed that the Co/Mo ratio of the slabs decreases to 0.4 *(Fig. 9)*. Considering the completion of the decoration of the MoS_2 slabs, this should imply an increase in the length up to 37 Å, a variation that has never been observed. Indeed, the TEM results showed that whatever the Co/Mo ratio, the length of the slabs is stable. It means that for the *CoMoP(0.7)-S* the slabs are not totally decorated, as a significant amount of Co is transformed into bulk cobalt sulfide, as shown by XPS. This may originate from the formation of Co_3O_4 on the oxide catalyst, but was not detected by XPS.

2.5 Activity Measurements

Figure 14 presents the hydrogenation activity expressed as the rate constant (in mole of converted toluene per mole of molybdenum and per hour) versus the Co/Mo atomic ratio for the CoMoP-type catalysts. It appears that the activity increases up to Co/Mo = 0.3 and reaches a plateau for higher ratios. Nevertheless, it would be interesting to prepare and test CoMoP catalysts with Co/Mo ratios of 0.8 and 0.9 in order to verify if the activity is stable or not for high Co/Mo ratios.

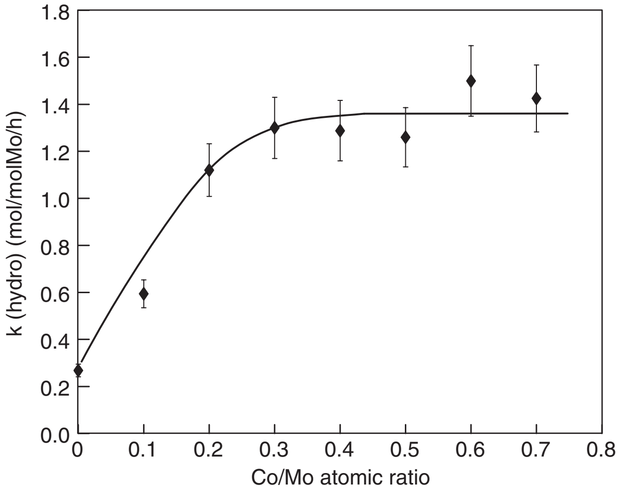

Figure 14

Catalytic activity in toluene hydrogenation of the sulfided CoMoP catalysts, at various Co/Mo ratios.

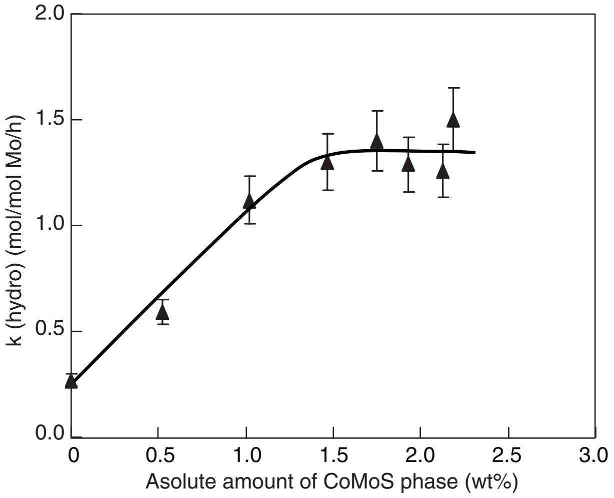

Figure 15

Toluene hydrogenation activity as a function of the CoMoS mixed phase amount detected by XPS for the sulfided CoMoP catalysts.

A direct correlation of the activity with the amount of active CoMoS was observed, as shown in Figure 15, which presents the toluene hydrogenation activity of the catalysts versus the amount of the CoMoS mixed phase as determined by the XPS quantification that we developed in this work. It seems that the MoS_2 slabs do not need to be fully decorated to present a maximum activity and should imply that all the CoMoS sites are not active. As it is now well recognized that activity of the CoMoP catalysts is closely related to the CoMoS mixed phase present on the surface, this shows the validity of the XPS quantification.

CONCLUSION

A decomposition of the XPS spectra of the CoMo-based HDS catalysts allowed us to obtain a quantitative analysis of the various entities present on the surface. Applied to a set of CoMoP-type catalysts with various Co/Mo atomic ratios, we showed that the amount of the active CoMoS mixed phase reaches a maximum for a Co/Mo ratio equal to 0.5, with 75% of the molybdenum transformed into MoS_2, whereas 50% to 60% of the initial cobalt is located in decoration of the MoS_2 slabs. Considering Kasztelan's geometrical model with a total substitution of the edge and corner molybdenum atoms, the length of the slab was deduced, the value being in agreement with the mean value deduced from the TEM characterizations. It means that all the MoS_2 slabs are completely decorated with Co atoms for a Co/Mo ratio equal to 0.5. The results of the toluene hydrogenation tests are in good agreement with the XPS quantitative analysis. Indeed, the maxima of hydrogenation activity are observed for Co/Mo ratios higher than 0.3, corresponding to the maximum amounts of the CoMoS mixed phase as evaluated by XPS. This shows that the toluene hydrogenation performance of a catalyst is a direct probe of the total amount of the CoMoS phase present in a CoMo catalyst. However, this study clearly shows that only 50% to 60% of the Co is implied in the mixed phase, suggesting that improvement of the catalytic performances is still possible with an increase in the Mo sulfidation.

REFERENCES

1 Topsøe H., Clausen B., Candia R., Wivel C., Mørup S. (1981) *In situ* Mössbauer emission spectroscopy studies of unsupported and supported sulfided Co-Mo hydrodesulfurization catalysts: evidence for and nature of a Co-Mo-S Phase. *J. Catal.*, **68**, 433-452.

2 Raybaud P., Hafner J., Kresse G., Kasztelan S., Toulhoat H. (2000) Structure, energetics, and electronic properties of the surface of a promoted mos2 catalyst: an *ab initio* local density functional study. *J. Catal.*, **190**, 128-143.

3 Griboval A., Blanchard P., Payen E., Fournier M., Dubois J.L. (1998) Alumina supported HDS catalysts prepared by impregnation with new heteropolycompounds. Comparison with catalysts prepared by conventional Co-Mo-P coimpregnation. *Catal. Today*, **45**, 277-283.

4 Griboval A. (1998) Synthèse d'hétéropolyanions à base de Co, Mo, P (Si). Préparation de catalyseurs d'hydrotraitement supportés sur alumine. *Thesis*, Université de Lille, France.

5 Iwamoto R., Grimblot J. (1999) Influence of phosphorus on the properties of alumina-basec hydrotreating catalysts. *Adv. Catal.*, **44**, 417-503.

6 http://www.casaxps.com.

7 Biesinger M.C., Brown C., Mycroft J.R., Davidson R.D., McIntyre N.S. (2004) X-ray photoelectron spectroscopy studies of chromium compounds. *Surf. Interface Anal.*, **36**, 1550-1563.

8 Grosvenor A.P., Kobe B.A., Biesinger M.C., McIntyre N.S. (2004) Investigation of multiplet splitting of Fe 2p XPS spectra and bonding in iron compounds. *Surf. Interface Anal.*, **36**, 1564-1574.

9 Martin C. (2003) Catalyseurs d'hydrodésulfuration préparés à partir d'hétéropolyanions de type Anderson. *Thesis*, Université de Lille, France.

10 Alstrup I., Chorkendorff I., Candia R., Clausen B.S. (1982) A combined X-ray photoelectron and Mössbauer emission spectroscopy study of the state of cobalt in sulfided, supported, and unsupported Co-Mo catalysts. *J. Catal.*, **77**, 397-409.

11 Echard M. (2001) Contribution à la connaissance des catalyseurs d'hydrotraitement CoMo/Al_2O_3: étude de la sulfuration et de l'adsorption d'H_2S sous flux et sous pression. *Thesis*, Université de Caen, France.

12 Bouwens S.M.A.M., van Veen J.A.R., Koningsberger D.C., de Beer V.H.J., Prins R. (1991) Extended X-ray absorption fine structure determination of the structure of cobalt in carbon-supported Co and Co-Mo sulfide hydrodesulfurization catalysts. *J. Phys. Chem.*, **95**, 123-134.

13 Nielsen L.P., Schønning M., Christensen S.V., Hoffmann S.V., Li Z., Hofmann P., Besenbacher F., Clausen B.S. (2001) Combined TPS, XPS, EXAFS, and NO-TPD study of the sulfiding of Mo/Al2O3. *Catal. Lett.*, **73**, 85-90.

14 Da Silva P. (1998) Influence de la taille des particules de MoS2 supportées sur alumine sur l'activité et la sélectivité des réactions d'hydrotraitement. *Thesis*, Université de Paris VI, France.

15 Portela L., Grange P., Delmon B. (1995) XPS and NO adsorption studies on alumina-supported Co-Mo catalysts sulfided by different procedures. *J. Catal.*, **156**, 243-254.

16 Galtayries A., Wisniewski S., Grimblot J. (1997) Formation of thin oxide and sulphide films on polycristalline molybdenum foils: characterization by XPS and surface potential variations. *J. Electron Spectrosc.*, **87**, 31-44.

17 Kasztelan S., Toulhoat H., Grimblot J., Bonnelle J.P. (1984) A geometrical model of the active phase of hydrotreating catalysts. *Appl. Catal.*, **13**, 127-159.

Final manuscript received in June 2006